ACS Catalysis

Research Article

pubs.acs.org/acscatalysis

Investigation of the Structure and Active Sites of TiO_2 Nanorod Supported VO_x Catalysts by High-Field and Fast-Spinning ^{51}V MAS NMR

Jian Zhi Hu,*[,†] Suochang Xu,[†,‡] Wei-Zhen Li,[†] Mary Y. Hu,[†] Xuchu Deng,[†] David A. Dixon,[§] Monica Vasiliu,[§] Raluca Craciun,[§] Yong Wang,[†,∥] Xinhe Bao,[‡] and Charles H. F. Peden[†]

[†]Institute for Integrated Catalysis and Fundamental and Computational Science Directorate, Pacific Northwest National Laboratory Richland, Washington 99354, United States

[‡]Dalian Institute of Chemical Physics, Chinese Academy of Sciences, Dalian 116023, People's Republic of China

[§]Department of Chemistry, The University of Alabama, Tuscaloosa, Alabama 35487-0336, United States

[∥]Voiland School of Chemical Engineering and Bioengineering, Washington State University, Pullman, Washington 99163, United States

Supporting Information

ABSTRACT: Supported VO_x/TiO_2-rod catalysts were studied by ^{51}V MAS NMR at high field using a sample spinning rate of 55 kHz. The superior spectral resolution allows for the observation of at least five vanadate species. The assignment of these vanadate species was carried out by quantum chemical calculations of ^{51}V NMR chemical shifts of model V surface structures. Methanol oxidative dehydrogenation (ODH) was used to establish a correlation between catalytic activity and the various surface V sites. It is found that monomeric V species are predominant at low vanadium loadings with two ^{51}V NMR peaks observed at about −502 and −529 ppm. V dimers with two bridged oxygens result in a peak at about −555 ppm. Vanadate dimers and polyvanadates connected by one bridged oxygen atom between two adjacent V atoms resonate at about −630 ppm. A positive correlation is found between the V dimers, giving rise to the −555 ppm peak, and the ODH rate, and an even better correlation is obtained by including V monomer contributions. This result suggests that surface V dimers related to the −555 ppm peak and monomers are the primary active sites for the methanol ODH reaction. Furthermore, a portion of the V species is found to be invisible to NMR and the level of such invisibility increases with decreasing V loading levels, suggesting the existence of paramagnetic V species at the surface. These paramagnetic V species are also found to be much less active in methanol ODH.

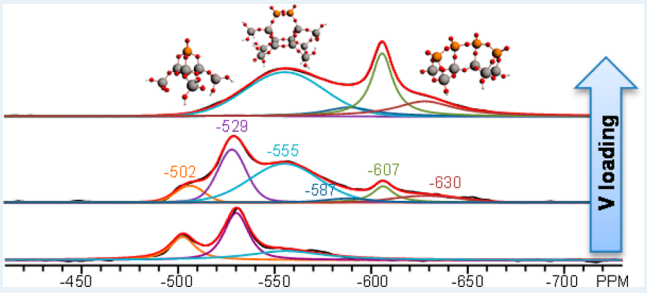

KEYWORDS: *^{51}V MAS NMR, chemical shift calculation, surface structure, catalytic active sites, NMR visibility of vanadium, methanol oxidative dehydrogenation reaction*

INTRODUCTION

Supported VO_x/TiO_2 catalysts are of considerable interest for their widespread applications in many important industrial processes, including the selective catalytic reduction of nitrogen oxides by ammonia[1,2] and the oxidative dehydrogenation (ODH) of light alkanes to alkenes and alkadienes.[3−5] This system is also a model for the analysis of interactions at the metal oxide/catalyst support interface.[6−10] Various techniques, including IR,[1,2,11,12] ESR,[11−13] X-ray absorption spectroscopy (EXAFS/XANES),[14−16] Raman,[2,17−19] NMR,[7,20−22] and computational modeling,[7−10] have been used to unravel the structure of the VO_x species on the supported catalysts. It has been proposed that supported vanadia species have distorted-tetrahedral coordination with a terminal V═O bond and bridging V−O−support and/or V−O−V bonds with the forms of monovanadate, polyvanadate, and crystalline V_2O_5. Obviously, the VO_4 tetrahedron can be strongly affected in the geometric and electronic structure by the nature of oxide supports, such as elemental identity, crystal phase, and even exposed facets. As a result, a significant difference in the catalytic activities usually arises. For example, the turnover frequencies (TOF) for the oxidation of methanol to formaldehyde vary in several orders of magnitude with varying oxides and vanadia loadings.[23] However, controversy still remains regarding the structures of such surface vanadium species, and the structure−reactivity relationship has yet to be established.

Received: February 10, 2015
Revised: April 13, 2015
Published: April 15, 2015

DOI: 10.1021/acscatal.5b00286
ACS Catal. 2015, 5, 3945−3952

Solid-state ^{51}V NMR is a powerful technique for the study of VO_x/TiO_2 catalyst systems. ^{51}V is a quadrupolar nucleus with quantum spin number $I = 7/2$ and natural abundance of 99.76%.[20] Note that vanadium in the V^{5+} oxidative state (i.e., vanadium in a singlet) is the only nuclei that can be observed by ^{51}V NMR. The quadrupolar coupling constant and asymmetry parameter can be directly obtained from the analysis of a ^{51}V NMR spectrum. These parameters are sensitive to subtle structural changes and have the potential to be used for investigating the detailed structures of surface vanadate. However, the existence of quadrupolar interactions and ^{51}V−^{51}V dipole interactions and chemical shift anisotropy (CSA) interactions in supported VO_x/TiO_2 catalyst result in significantly broadened NMR peaks for the various vanadate sites. Such line broadening causes severe superposition of peaks from different V environments, and renders a static ^{51}V NMR spectrum very difficult to analyze, even unusable in the cases of simultaneous existence of multiple V sites (see ref 20 and references therein). Using the technique of magic angle spinning (MAS), one is able to narrow the lines by averaging dipolar chemical shift anisotropy and first order quadrupolar effects. However, in the ^{51}V NMR spectra of supported VO_x/TiO_2 catalysts, MAS at common spinning rates is not sufficient to separate the centerband spectra from the associated spinning sidebands (SSBs) or to separate the SSBs of different vanadate sites.[20,21] Recent developments in MAS probe technology have enabled a considerable increase in sample spinning rate which, in principle, allows for the definitive separation of all of the centerbands from their associated SSBs. The only successful example in the study of supported VO_x/TiO_2 catalysts has been demonstrated recently by using a sample spinning rate of 35 kHz at a magnetic field of 9.7 T.[7] Since the second-order quadrupolar interaction scales inversely with the applied magnetic field, it is expected that, at higher magnetic fields, the resolution of the centerband spectra will be even further improved. Therefore, a higher spectral resolution and hence more detailed structural information on surface V species can be obtained at increased magnetic field. However, the spectral width associated with the CSA interaction is proportional to the magnetic field, meaning that, at magnetic fields higher than 9.7 T, a spinning rate higher than 35 kHz is required to get high-resolution spectra.

Herein, the ^{51}V solid-state (SS) MAS NMR spectra at a high magnetic field of 19.975 T under a fast sample spinning rates of 55 kHz were obtained to study supported VO_x/TiO_2-rod catalysts at various VO_x loadings ranging from 0.2% to 5% by weight. The experimental work in combination with quantum chemical electronic structure calculations enabled a relationship between different surface V sites and the catalytic activity of methanol ODH reaction to be established.

EXPERIMENTAL SECTION

Sample Preparation. Rodlike titania catalyst support materials (TiO_2 rods) were prepared by the following procedures.[24] Typically, 10 mL (0.03 mol Ti) of tetra-*n*-butyltitanate (TNBT, Alfa Aesar, 99%) was slowly added to 300 mL of deionized water with magnetic stirring, and the mixture was stirred overnight at room temperature. The resulting white precipitate [$Ti(OH)_4$] was centrifugally separated from the solution and washed with deionized water three times. The resulting titanium hydroxide was dispersed in 200 mL of deionized water. The pH of the fresh obtained suspension was adjusted to 9 by adding ammonium solution. With the addition of 100 mL of hydrogen peroxide (H_2O_2; Alfa Aesar, 27%), the suspension changed to an orange transparent solution of peroxotitanium acid. For such peroxotitanium acid solution, the concentration of Ti^{4+} was 0.1 mol/L, the molar ratio of $[H_2O_2]/[Ti^{4+}]$ was 25, and the pH was about 2. Each 100 mL of peroxotitanium acid solution was transferred into a 125 mL Teflon-lined vessel which was then set into an autoclave and heated at 90 °C for 3 days, followed by heating at 120 °C for 2 days, and finally at 150 °C for 2 days for better crystallization. After hydrothermal treatment, the resulting precipitate was centrifugally separated and dried at 110 °C in ambient air overnight and finally calcined at 400 °C for 5 h to obtain TiO_2 rods. The TiO_2 rods are 10−20 nm in diameter and 50−100 nm in length with pure anatase phase and have a surface area of 57.5 m^2/g.

Supported vanadia catalysts were prepared by incipient wetness impregnation of the TiO_2 rods with NH_4VO_3 (Alfa Aesar, 99.99%) in saturated aqueous oxalic acid solution at room temperature for 20 h. Impregnated supports were dried at 110 °C in static ambient air overnight and then calcined at 400 °C for 5 h. The prepared samples were subsequently transferred to a nitrogen glovebox and packed into an airtight MAS rotor under an anhydrous atmosphere for ^{51}V MAS NMR measurements. These samples are labeled as xV/TiO_2, where x is the vanadia weight loading in units of weight percent. Three vanadia weight loadings were studied (x = 0.2, 0.9, 5), which correspond to 3%, 10%, and 86% surface coverages of TiO_2 rod supports by vanadia, respectively, by assuming that all of the VO_x forms a two-dimensional layer on the TiO_2-rod surface and the monolayer V surface density is 7 V/nm^2.

Reaction Testing. Methanol ODH reactions were carried out at atmospheric pressure in a fixed-bed microreactor. Catalyst powders (~10 μmol VO_x, 60−80 mesh), diluted with SiC powder (3 g, 60−80 mesh) to prevent temperature gradients, were held at the middle of a quartz reactor (10 mm i.d., catalyst bed height ~30 mm) between two layers of quartz wool. A *K*-type thermocouple lined with a quartz tube was inserted into the catalyst bed to measure and control the temperature. The catalysts were pretreated in an air flow at 400 °C for 30 min before cooling to the reaction temperature (280 °C). Methanol was introduced into the reactor by flowing pressurized zero air through a saturator maintained at 50 °C and then a cooled-water condenser. The concentration of methanol was kept at 4% (molar ratio) by controlling the condenser temperature in a range of 2−5 °C with a cryostat (Fisher, Isotemp 1016D) to make up for the change in methanol partial pressure induced by varying the air flow rates required to maintain methanol conversions at ~15%. The outlet of the reactor to the six-way gas sampling valve was heated at 150 °C to avoid condensation of the products. Only ~50 mL/min of outlet gas passed through the sample loop and the remaining gas was vented to avoid the pressure buildup in the reactor. Reactants and products were analyzed by an online gas chromatograph (Agilent 7890A) equipped with an isolation system for molecular sieve 5A and a HayeSep T packed columns, and a thermal conductivity detector. Selectivities are reported on a carbon basis as the percentages of the converted methanol appearing as a given product. Rates for the primary methanol oxidative dehydrogenation (ODH) reaction to HCHO are reported as the combined molar formation rates for HCHO, CH_3OCH_3 (DME), $HCOOCH_3$, and CO_2 per surface VO_x, because each product formation requires one oxidative methanol dehydrogenation event.

DOI: 10.1021/acscatal.5b00286
ACS Catal. 2015, 5, 3945−3952

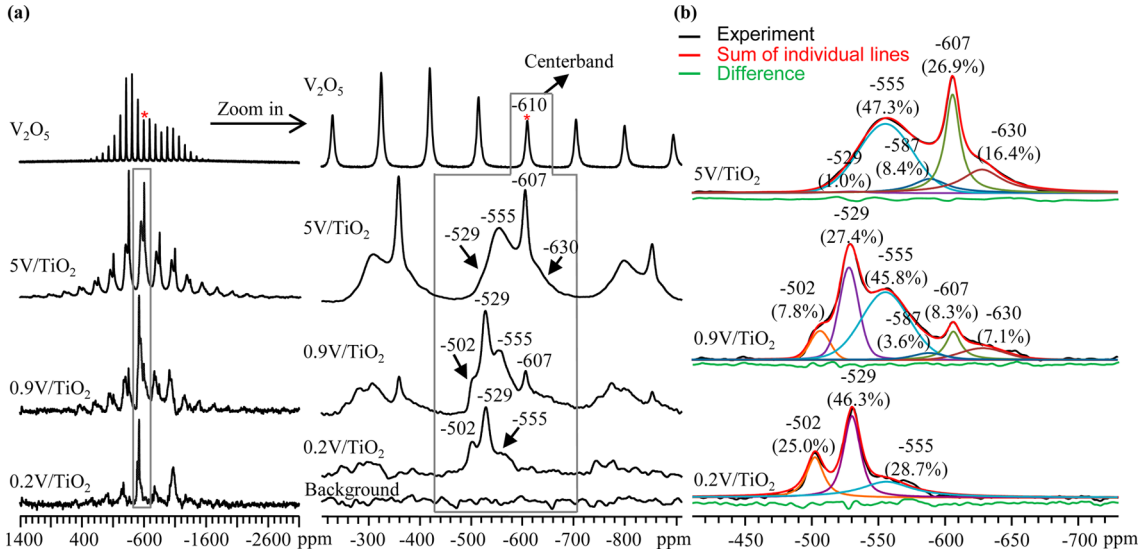

Figure 1. (a) Fast sample spinning (55 kHz) solid state ^{51}V MAS NMR spectra of supported VO$_x$/TiO$_2$ rod catalysts with different V_2O_5 loadings. For 0.2V/TiO$_2$, 0.9V/TiO$_2$, and 5V/TiO$_2$, total scan numbers were 510000, 330000, and 180000, respectively. The spectrum for a V_2O_5 powder was acquired at 21 kHz with a recycle delay at 1 s and 32 scans. Highlighted inside the rectangular box are the centerband spectra, which are also shown in zoom-in spectra to the right. (b) Decompositions of the ^{51}V MAS centerband NMR spectra. The chemical shift of the peak center and the percentage of the peak area normalized to the total peak area of the centerband spectra are presented at the top of each deconvoluted peak.

NMR Measurements. All of the ^{51}V NMR experiments were performed at room temperature on a Varian-Inova 850 MHz NMR spectrometer, operating at a magnetic field of 19.975 T. The corresponding Larmor frequency was 223.367 MHz. The ultra-wide ^{51}V MAS NMR spectra were acquired with a rotor-synchronized Hahn echo (with the half echo time τ = 1 rotor period) pulse sequence at rf field strengths of 143 kHz and a spectral width of 5 MHz at a sample spinning rate of 55 kHz, using a commercial 1.2 mm pencil-type MAS probe. Depending on the samples, 180000−510000 scans with a 0.2 s recycle delay were used. All spectra were externally referenced using the centerband of bulk V_2O_5 as the secondary reference: i.e., −610 ppm with respect to the common reference of $VOCl_3$ (0 ppm).

Quantum Chemistry Calculations. Electronic structure calculations were performed using the Amsterdam Density Functional (ADF) package.[25−27] The generalized gradient approximation (GGA) based Becke−Lee−Yang−Parr function (BLYP)[28,29] with dispersion functions (BLYP-D)[30] was employed for geometry optimization. All calculations were performed using the TZ2P basis set (triple ζ, two polarization function, all-electron) with Slater type functionals[31] implemented in ADF. NMR chemical shift calculations were performed on the basis of the geometry-optimized structures at the same level of theory and with the same basis set to evaluate the chemical shielding for each atom.

For the calculation of the ^{51}V NMR chemical shift, a standard reference is needed. We chose to use a model of V_2O_5 as a reference as follows. A cluster containing eight vanadate atoms was extracted from the crystal structure of V_2O_5 from the American Mineralogist Crystal Structure Database,[32] and the geometries of the atoms were frozen while terminal oxygen atoms were charge balanced by adding hydrogen atoms. Only the positions of the hydrogens were optimized prior to NMR calculations. NMR calculations were then performed on the frozen geometry V_2O_5 cluster with optimized hydrogen atom positions (Figure S1 in the Supporting Information), and the absolute chemical shift of the center vanadate atom, which should closely mimic the bulk V_2O_5 coordination, was employed as the reference. The calculated isotropic shielding for this V site was −1341.2 ppm. Since bulk V_2O_5 is located at −610 ppm experimentally with reference to $VOCl_3$, the calculated shielding for a V site in the model cluster is converted to the observed chemical shift with reference to $VOCl_3$ (0 ppm) according to $\delta_{obs} = \delta(V_2O_5) - \delta_{calc} - 610$ (ppm) = $-1341.2 - \delta_{calc} - 610$ (ppm). This approach, i.e., using a standard with a structure quite similar to that of the proposed surface vanadate species, helps to suppress systematic errors associated with directly using the calculated absolute isotropic shielding from a single $VOCl_3$ molecule as the chemical shift reference. The NMR calculations were performed in the gauge invariant atomic orbital (GIAO) approach[33] at the DFT level on the basis of developments from the Ziegler group with the same function and basis set as those for geometry optimization.[34−37]

RESULTS AND DISCUSSION

Experimental NMR Chemical Shifts. Figure 1 shows the ^{51}V MAS (55 kHz) NMR spectra of the supported VO$_x$/TiO$_2$ rod catalysts with different loadings of V_2O_5: i.e., 0.2, 0.9, and 5 wt %. For comparison, the ^{51}V MAS (21 kHz) spectrum of bulk V_2O_5 is shown in the top trace, where the centerband peak labeled with an asterisk is that used as the chemical shift reference at −610 ppm. The centerband of bulk V_2O_5 is a symmetric peak, with the second-order quadrupolar effect on the line shape being difficult to observe, indicating that, at high magnetic fields, the effect of line broadening due to quadrupolar interactions is reduced as expected. In fact, the sideband pattern can be nicely fit with only contributions from the CSA. The goodness of the fit using principal values of δ_{11} −82 ± 5 ppm, δ_{22} −410 ± 5 ppm, and δ_{33} −1338 ± 5 ppm are provided in Figure S2 in the Supporting Information, where it clearly shows that, at high field, the effect of the second-order quadrupolar interaction on the line shape can be ignored. It should be noted that the principal values determined from this work are noticeably different from those of a previous literature

DOI: 10.1021/acscatal.5b00286
ACS Catal. 2015, 5, 3945−3952

Table 1. Normalized Peak Intensities, in Total ^{51}V MAS NMR Integrated Spectral Areas, for the Supported VO_x/TiO_2-Rod Catalysts[a]

		peak area of each line (au)						
sample	sample weight (mg)	−502 ppm	−529 ppm	−555 ppm	−587 ppm	−607 ppm	−630 ppm	visibility of V species (%)
0.2V/TiO_2	2.7	25	46	29	NA	NA	NA	20.3
0.9V/TiO_2	2.3	61	213	357	28	65	55	35.2
5V/TiO_2	2.5	NA	118	5518	980	3139	1915	95.0

[a]The last column shows the visibility of the loaded vanadium from spin counting experiments (i.e., the percentage of V^{5+} over the total amount of loaded vanadia).

Table 2. Site Fractions of Different Vanadia Species, in Total Vanadia Loading, for the Three VO_x/TiO_2 Rod Samples and Their ODH Reaction Rates

	site fractions in total vanadia loading						
sample	−502 ppm	−529 ppm	−555 ppm	−587 ppm	−607 ppm	−630 ppm	ODH rate per V atom (s^{-1})
0.2V/TiO_2	0.051	0.094	0.058	0	0	0	0.097
0.9V/TiO_2	0.028	0.096	0.161	0.013	0.029	0.025	0.160
5V/TiO_2	0	0.010	0.449	0.080	0.256	0.156	0.202

report,[20] where δ_{11} −310 ppm, δ_{22} −310 ppm, and δ_{33} −1270 ppm were reported. Due to the goodness of the fit of the SSBs using just the pure chemical shift anisotropy, and the negligible contribution from the second-order quadrupolar interaction that also simplifies the fit, the results from the present study should be more accurate than those previously reported.[20]

At the fast sample spinning rate of 55 kHz, the peaks in the centerband spectra of the synthesized catalysts are successfully separated from their associated SSBs. Furthermore, when a high magnetic field of 19.975 T is employed, the spectral resolution of the centerband spectra is significantly improved (see the zoom-in spectra on the right-hand side of Figure 1a) in comparison with those reported previously in similar systems but at a much lower magnetic field of 9.7 T.[7] The line shape of the centerband spectra (Figure 1a) varies with increasing loading of vanadia, indicating changes in the distribution of various surface vanadate species in these supported catalysts. For the sample 0.2V/TiO_2, only three peaks at about −502, −529, and −555 ppm were observed. In 0.9V/TiO_2, an additional resonance appears at about −607 ppm, which is close to the centerband peak position of bulk V_2O_5 (i.e., −610 ppm, Figure 1a). In 5V/TiO_2, the relative intensity of the −607 ppm peak is increased accompanied by a significant increase in relative intensity of the −555 ppm peak. Furthermore, the peaks at −555, −529, and −502 ppm become broader in comparison with those at the 0.2 and 0.9 wt % loadings. An additional shoulder peak centered at about −630 ppm is also observed in 5 V/TiO_2.

To gain further insight into the peak changes as a function of V_2O_5 loading, the centerband spectra are fit using a set of peaks centered at about −502, −529, −555, −607, and −630 ppm, as illustrated in Figure 1b for 0.2V/TiO_2 and 0.9 V/TiO_2. In 5V/TiO_2, the −502 ppm peak is difficult to observe while the −529 ppm peak is still visible as a shoulder peak that is sitting on the side of the −555 ppm peak. An extra peak at about −587 ppm is needed in order to fit both 0.9V/TiO_2 and 5V/TiO_2 well. The relative percentages of the various peaks in the centerband spectra are also given in Figure 1b. By integration of the entire spectrum for each sample in Figure 1a, the absolute integrated spectral intensity relative to a fixed spectrometer intensity reference is obtained. Such intensity is further scaled per unit weight (mg) and per unit number of scans so that integrated peak intensities from samples with different V_2O_5 loadings can be directly compared. This strategy is based on the fact that the tuning and match conditions of the probe were set exactly the same from sample to sample so that the peak intensity is jointly proportional to the weight of the sample and the total accumulation number used for acquiring a spectrum. Multiplying the relative percentage by the normalized total integrated spectral intensities for each sample, the normalized peak intensity for each peak is obtained, and the results are summarized in Table 1. Since bulk V_2O_5 is 100% visible by ^{51}V NMR, we used it as a spin-counting reference standard, and we found that approximately 95.0% of the ^{51}V spins from 5V/TiO_2 were observed while only about 20.3% and 35.2% of ^{51}V spins were observed in 0.2V/TiO_2 and 0.9V/TiO_2, respectively. This result shows that, at a low level of V_2O_5 loading, a significant amount of V is invisible by NMR and suggests the presence of paramagnetic V species. In combination with EPR measurements (Figure S3 in the Supporting Information), these invisible V species can be assigned to V^{4+}.

The results in Table 1 allow the peak intensities to be compared quantitatively between samples with different V_2O_5 loadings. As the peak intensity is proportional to the number of V sites, it is clearly indicated that the number of V sites corresponding to each peak, i.e., −555, −587, −607, and −630 ppm, initially increases with V_2O_5 loading. In particular, the absolute peak intensity or the number of V sites for the −555 ppm peak increases dramatically with V_2O_5 loading; i.e., by about 12- and 192-fold for 0.9V/TiO_2 and 5V/TiO_2, respectively, in comparison with that of 0.2V/TiO_2. It is worth noting that the reaction rate data for methanol ODH is expressed as the ODH rate per V atom (s^{-1}). To better correlate with the ODH rate, we collected (Table 2) the percentage of each V species associated with each ^{51}V spectral peak (V^{5+}) relative to the total V species by including the NMR-invisible V species (V^{4+}).

The assignments of the various peaks are quite challenging due to the technical limitations from the prior literature NMR studies:[7,22,38,39] i.e., the severe overlap of the resonant peaks from different V species due to the use of a relatively low magnetic field, the relatively low sample spinning rates utilized, and the lack of a suitable set of standard samples that closely mimic the possible surface V structures on the TiO_2 surface. Nevertheless, the results from the literature may be used as a starting place for discussing spectral assignments.

DOI: 10.1021/acscatal.5b00286
ACS Catal. 2015, 5, 3945−3952

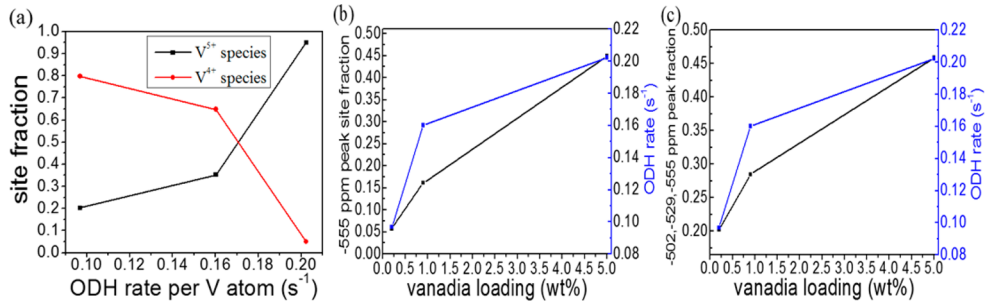

Figure 2. Correlation of methanol ODH rates with different vanadia species: (a) V^{5+} and V^{4+} species; (b) −555 ppm peak; (c) sum of the −502, −529, and −555 ppm peaks.

Table 3. Calculated ^{51}V Chemical Shifts in ppm with the V_2O_5 Cluster as a Secondary Reference to $VOCl_3$ (0 ppm)[a]

Model surface V-species after geometry optimization (V, Ti, O, H)	Cluster Formula	Calc	Expt	Structure Label
	$OVO_3(TiO(OH))_3$	-494	-502	**A1**
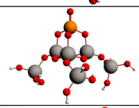	$OVO_3(TiO(OTi(OH)_3)_3$	-496	-502	**A2**
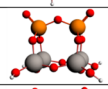	$V_2O_7(TiO(OH))_4$	-646	-630	**B1**
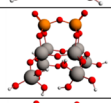	$V_2O_7(TiO((OTi(OH)_3))_4$	-639	-630	**B2**
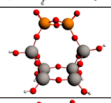	$V_2O_6(TiO(OH))_4$	-548	-555 -529	**C1**
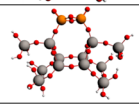	$V_2O_6(TiO((OTi(OH)_3))_4$	-553	-555	**C2**
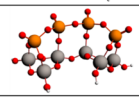	$V_4O_{13}O(TiO_3(TiOH)_2)_2$	-641 -653 -636 -623	-630	**D**
	$V_4O_{12}(TiO(OH))_4$	-544 -702	-555 -630	**E1**
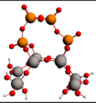	$V_4O_{12}(TiO((OTi(OH)_3))_4$	-530 -665	-529 -630	**E2**

[a]The calculated shifts are converted to the observed chemical shift scale by $\delta_{obs} = -1341.2 - \delta_{calc} - 610$ (ppm).

The −555 ppm peak was originally suggested to be V^{5+} in a distorted-tetrahedral environment on the basis of low-field and low-speed ^{51}V MAS NMR and static ^{51}V NMR studies.[22] Luca et al.[38] attributed a peak at −530 ppm to tetrahedral V^{5+} as well, but similar peaks were typically observed in model compounds with a distorted-octahedral structure in the work of Eckert and Wachs.[22] Eckert and Wachs experimentally detected peaks at −510 and −550 ppm in their VO_x/TiO_2 samples by acquiring a series of spectra with varied moderate sample spinning rates at low magnetic field. Although the identification of the peaks was very difficult, it seems likely that the centerband peaks at −510 and −550 ppm were detected in their VO_x/TiO_2 samples. These authors suggested an assignment of the −510 and −550 ppm peaks to octahedral and tetrahedral V^{5+} environments, respectively, on the basis of their model compound studies. In a work by Borovkov et al.,[7] a peak at −530 ppm was assigned to V^{5+} ions with trigonal pyramid coordination: i.e., a highly distorted tetrahedral structure where the bond length for the double-bonded oxygen is significantly stretched. Given the very ambiguous assignments in the literature, it is difficult to assign our −529 ppm to the V with either tetrahedral or octahedral site symmetry without additional information. Likewise, it is

DOI: 10.1021/acscatal.5b00286
ACS Catal. 2015, 5, 3945−3952

also very difficult to definitively assign the −502 ppm peak only on the basis of the literature. The wide shoulder peak centered at about −630 ppm, which overlapped with the signal at −607 ppm and has been previously suggested to be disordered octahedral V^{5+} ions strongly interacting with the surface of titania,[7,40] also remains difficult to assign. The only peak that can be assigned with confidence is the −607 ppm sharp peak. Since the −607 ppm peak is very close to the centerband shift of bulk V_2O_5, it is assigned as three-dimensional V_2O_5 structures on the surface or V_2O_5 micro- or nano-sized particles on the basis of both the sharpness of the peak and the similarity of the chemical shift to that of bulk V_2O_5. More discussion of ^{51}V NMR peak assignments will be given below, on the basis of calculated NMR chemical shifts.

ODH Rates. Figure 2a indicates a positive correlation between the percentage of V^{5+} and the methanol ODH rate, while a negative correlation exists between the ^{51}V NMR invisible (i.e., the V^{4+}) species and methanol ODH rate. This strongly suggests that the V^{5+} species are the catalytic active centers mainly responsible for the observed methanol ODH when VO_x/TiO_2 are used as catalysts, consistent with prior conclusions that V^{4+} sites have much lower activity than V^{5+} sites.[41]

It has been reported that monomeric and polymeric vanadia and even the bulk V_2O_5 are catalytically active.[41] Since there are six V^{5+} surface species observed by ^{51}V MAS NMR, the next question is as follows: what surface V^{5+} species are mainly responsible for the methanol ODH reaction in this study? Figure 2b,c and Figure S4 in the Supporting Information summarize multiple correlations between the percentages of the various V sites, related to different ^{51}V peaks relative to the total V loading (both NMR visible and invisible), and the ODH reaction rate. There is a clear negative correlation between the −502 ppm peak, the −529 ppm peak, or the sum of the −502 and −529 ppm peaks and the ODH rate (Figure S4). Such a negative correlation is due to the decreased percentage of these two V species with increased V_2O_5 loading relative to the total observable ^{51}V species. Although this result certainly shows that the total amount of V species associated with both the −502 and the −529 ppm peaks are not the major surface V species responsible for the observed methanol ODH rate over catalysts with V_2O_5 loadings from 0.2 to 5 wt %, it does not tell us how active these two V species are. In contrast, there is a positive correlation if only the −555 ppm peak is used, indicating that the V species associated with the −555 ppm peaks are the major surface V sites responsible for the observed methanol ODH rate. However, an even better correlation between the V sites related to the (−555 ppm) + (−502 ppm) + (−529 ppm) peaks is observed, while adding the peaks of −587, −607, and −630 ppm did not improve the correlation with the observed methanol ODH rate (see Figure S4). These results suggest that the total V sites corresponding to the −555, −502, and −529 ppm peaks are likely the most catalytically active sites for CH_3OH ODH.

Computational NMR Chemical Shifts. To gain insight into the structures of titania-supported V species, computational modeling of the ^{51}V isotropic chemical shifts was carried out. Various clusters of VO_x/TiO_x were constructed to simulate a number of possible surface monovanadate and polyvanadate structures, with the oxygen atoms shared with TiO groups initially terminated by a hydrogen. The geometries were fully optimized, and the ^{51}V isotropic chemical shifts were calculated at these geometry-optimized structures (Table 3). On comparison of structures **A1** and **A2**, we can see that for monomeric tetrahedral vanadate species with one doubly bonded oxygen and three V−O−Ti bonds, the calculated isotropic ^{51}V chemical shifts, −494 and −496 ppm, are close to the −502 ppm experimental peak. On the basis of this prediction, we can assign the peak at −502 ppm to monomeric tetrahedral vanadate species that are anchored on the anatase surface via three V−O−Ti bonds.

For vanadium dimers **B1** and **B2**, each V atom is doubly bonded to an oxygen and singly bonded to three additional oxygens, one oxygen atom of which is bridging between two V atoms. For the V sites in both structures, the calculated ^{51}V isotropic chemical shifts are located at about −646 to −639 ppm. The peak centered at about −630 ppm found from both $0.9V/TiO_2$ and $5V/TiO_2$ in Figure 1b is in good agreement with the calculated values. Thus, assignment of the −630 ppm peak to V dimer structures with an oxygen bridge between the two V sites is suggested. Similar to the V monomer case, the additional −OTi groups in **B2** give slightly better agreement with the experimental value. Linear polyvanadate with one bridging oxygen atom between adjacent two V sites in the cluster, such as those in **D**, have predicted ^{51}V isotropic chemical shifts at −623, −636, −641, and −653 ppm, respectively. These values are also close to the experimental value of −630 ppm. Considering that the experimental peak centered at −630 ppm is broad, the −630 ppm peak should also have a contribution from V atoms in linear two-dimensional polyvanadate structures.

Cluster models **C1** and **C2** show another type of vanadium dimer where two oxygen atoms form a pair of bridges between the two V sites. For this type of V dimer, an isotropic ^{51}V chemical shift between −548 and −553 ppm is predicted. As this value is very close to the −555 ppm peak observed in Figure 1, we assign this peak to V dimers with a pair of oxygen bridges between the two V sites. The peak located at about −529 ppm lies at approximately the midpoint between the −502 and the −555 ppm peaks, and it is difficult to assign this −529 ppm peak on the basis of the cluster models that were used here. Although the two-layer cluster model **E2** has a predicted isotropic shift at −530 ppm for the top two V sites that are linked together with two bridged oxygen atoms, the chemical shifts of the two V sites in the second layer are predicted to be −665 ppm and there are no experimental peaks in this region (Figure 1). Instead, we believe that the −529 ppm peak is likely to be related to a monomeric V species on the basis of the fact that this peak, like the −502 ppm peak, has a negative correlation with the methanol ODH reaction rate as discussed above. Because the −529 ppm peak is the dominant peak at a low loading of catalysts, it may be related to a substitutional V site (for a defect missing Ti), but additional investigations are needed to clarify this hypothesis. Finally, the small peak located at about −587 ppm present at high V loadings lies between the peaks at about −555 and −630 ppm and, thus, could be due to V dimer or linear polyvanadate structures.

CONCLUSIONS

In this work, supported VO_x/TiO_2 rod catalysts were studied by solid-state ^{51}V MAS NMR at a high magnetic field of 19.975 T using a fast sample spinning rate of 55 kHz. The achieved superior spectral resolution, for the first time, allows for the observation of at least five vanadate species with peaks centered at approximately −502, −529, −555, −587, and −603 ppm and

DOI: 10.1021/acscatal.5b00286
ACS Catal. 2015, 5, 3945−3952

a broad peak at −630 ppm, respectively. Quantum chemical calculations of the isotropic ^{51}V NMR chemical shifts at the density functional theory level on model V surface structures were carried out to gain insight into the detailed structures and the possible assignments of the observed NMR features to various surface vanadate species. A catalytic reactivity test of CH_3OH ODH was used to establish a possible connection between the ODH reaction rates and the various surface V species in order to identify the catalytically active sites. It is found that monomeric V species dominate the catalyst at low V loading, where two peaks are observed at about −502 and −529 ppm, respectively. V dimers are assigned to the −555 and −630 ppm peaks, respectively, depending on whether the structure has one oxygen atom acting as a single-bond bridge between the two V sites (−630 ppm) or the structure has two oxygen atoms acting as two separate bridges between V atoms (−555 ppm). Linearly structured polyvanandates with only one bridging oxygen atom between two adjacent V sites also contribute to the −630 ppm peak. A positive correlation is found between the V dimers related to the −555 ppm peak and the ODH rate, while an improved correlation is obtained by adding the contributions from the monomers related to both the −502 and the −529 ppm peaks. This result indicates that surface V dimers (−555 ppm) and V monomer species (−502 and −529 ppm) are the major active sites for ODH. However, the percentage of monomeric species decreases significantly with an increase in V loading, rendering the monomeric species a decreasing role in the overall observed methanol ODH rates at high V loadings. The visibility of V species was determined by quantifying ^{51}V MAS NMR spectra, demonstrating that a (sometimes significant) portion of the V species is invisible by ^{51}V MAS NMR. In particular, the level of such invisibility increases with decreased V loading levels, suggesting the existence of paramagnetic V species at low surface coverages. A negative correlation between the ODH rate and the invisible V species is obtained, suggesting that paramagnetic V species are much less active (perhaps even inactive) for the ODH reaction.

■ ASSOCIATED CONTENT

Supporting Information

The following file is available free of charge on the ACS Publications website at DOI: 10.1021/acscatal.5b00286.

Optimized V_2O_5 cluster (Figure S1), simulated spectrum of V_2O_5 ^{51}V MAS spectrum at 21 kHz (Figure S2), EPR spectra of TiO_2 rrod support and VO_x/TiO_2 rod catalysts (Figure S3), correlation between the percentages of a surface vanadate species related to a ^{51}V MAS NMR centerband peak and the methanol ODH rate (Figure S4), and the optimized geometries for the models given in Table 3 of the paper (Table S1) (PDF)

■ AUTHOR INFORMATION

Corresponding Author

*J.Z.H.: e-mail, Jianzhi.Hu@pnnl.gov; fax, (509) 371-6546; tel, (509) 371-6544.

Notes

The authors declare no competing financial interest.

■ ACKNOWLEDGMENTS

This research was supported by the U.S. Department of Energy (DOE), Office of Basic Energy Sciences, Division of Chemical Sciences, Biosciences and Geosciences. All of the NMR experiments were performed in the Environmental Molecular Sciences Laboratory (EMSL), a national scientific user facility sponsored by the DOE's Office of Biological and Environmental Research and located at Pacific Northwest National Laboratory (PNNL). Computational modeling was carried out using EMSL's supercomputers. PNNL is a multi-program national laboratory operated for the DOE by Battelle Memorial Institute under Contract DE-AC06-76RLO 1830. Dr. Eric D. Walter is acknowledged for his help with the EPR measurement. Dr. Ju Feng is acknowledged for his assistance in packing samples for NMR experiments, and Dr. Zhenchao Zhao is acknowledged for his assistance in preparing this paper. D. A. Dixon acknowledges the Robert Ramsay Chair fund for partial support.

■ REFERENCES

(1) Topsoe, N. Y.; Topsoe, H.; Dumesic, J. A. *J. Catal.* **1995**, *151*, 226−240.
(2) Amiridis, M. D.; Wachs, I. E.; Deo, G.; Jehng, J. M.; Kim, D. S. *J. Catal.* **1996**, *161*, 247−253.
(3) Cavani, F.; Trifiro, F. *Catal. Today* **1995**, *24*, 307−313.
(4) Boisdron, N.; Monnier, A.; Jalowieckiduhamel, L.; Barbaux, Y. *J. Chem. Soc., Faraday Trans.* **1995**, *91*, 2899−2905.
(5) Blasco, T.; Nieto, J. M. L. *Appl. Catal., A* **1997**, *157*, 117−142.
(6) Della Negra, M.; Sambi, M.; Granozzi, G. *Surf. Sci.* **1999**, *436*, 227−236.
(7) Borovkov, V. Y.; Mikheeva, E. P.; Zhidomirov, G. M.; Lapina, O. B. *Kinet. Catal.* **2003**, *44*, 710−717.
(8) Jug, K.; Nair, N. N.; Bredow, T. *Surf. Sci.* **2005**, *596*, 108−116.
(9) Nair, N. N.; Bredow, T.; Jug, K. *J. Phys. Chem. B* **2005**, *109*, 12115−12123.
(10) Calatayud, M.; Minot, C. *Top. Catal.* **2006**, *41*, 17−26.
(11) Busca, G.; Centi, G.; Marchetti, L.; Trifiro, F. *Langmuir* **1986**, *2*, 568−577.
(12) McGregor, J.; Huang, Z.; Shiko, G.; Gladden, L. F.; Stein, R. S.; Duer, M. J.; Wu, Z.; Stair, P. C.; Rugmini, S.; Jackson, S. D. *Catal. Today* **2009**, *142*, 143−151.
(13) Lapina, O. B.; Shubin, A. A.; Nosov, A. V.; Bosch, E.; Spengler, J.; Knozinger, H. *J. Phys. Chem. B* **1999**, *103*, 7599−7606.
(14) Kozlowski, R.; Pettifer, R. F.; Thomas, J. M. *J. Chem. Soc., Chem. Commun.* **1983**, 438−439.
(15) Rodella, C. B.; Mastelaro, V. R. *J. Phys. Chem. Solids* **2003**, *64*, 833−839.
(16) Lin, H. M.; Kao, S. T.; Lin, K. M.; Chang, J. R.; Shyu, S. G. *J. Catal.* **2004**, *224*, 156−163.
(17) Wu, Z.; Stair, P. C.; Rugmini, S.; Jackson, S. D. *J. Phys. Chem. C* **2007**, *111*, 16460−16469.
(18) Nieto, J. M. L.; Kremenic, G.; Fierro, J. L. G. *Appl. Catal.* **1990**, *61*, 235−251.
(19) Weckhuysen, B. M.; Keller, D. E. *Catal. Today* **2003**, *78*, 25−46.
(20) Lapina, O. B.; Mastikhin, V. M.; Shubin, A. A.; Krasilnikov, V. N.; Zamaraev, K. I. *Prog. Nucl. Magn. Reson. Spectrosc.* **1992**, *24*, 457−525.
(21) Nielsen, U. G.; Topsoe, N. Y.; Brorson, M.; Skibsted, J.; Jakobsen, H. J. *J. Am. Chem. Soc.* **2004**, *126*, 4926−4933.
(22) Eckert, H.; Wachs, I. E. *J. Phys. Chem.* **1989**, *93*, 6796−6805.
(23) Deo, G.; Wachs, I. E. *J. Catal.* **1994**, *146*, 323−334.
(24) Gao, Y.; Luo, H.; Mizusugi, S.; Nagai, M. *Cryst. Growth Des.* **2008**, *8*, 1804−1807.
(25) Guerra, C. F.; Snijders, J. G.; te Velde, G.; Baerends, E. J. *Theor. Chem. Acc.* **1998**, *99*, 391−403.
(26) te Velde, G.; Bickelhaupt, F. M.; Baerends, E. J.; Guerra, C. F.; Van Gisbergen, S. J. A.; Snijders, J. G.; Ziegler, T. *J. Comput. Chem.* **2001**, *22*, 931−967.
(27) *ADF2014*; SCM, Theoretical Chemistry, Vrije Universiteit, Amsterdam, The Netherlands; http://www.scm.com.

DOI: 10.1021/acscatal.5b00286
ACS Catal. 2015, 5, 3945−3952

(28) Lee, C. T.; Yang, W. T.; Parr, R. G. *Phys. Rev. B: Condens. Matter Mater. Phys.* **1988**, *37*, 785−789.
(29) Becke, A. D. *Phys. Rev. A: At., Mol., Opt. Phys.* **1988**, *38*, 3098−3100.
(30) Grimme, S.; Antony, J.; Schwabe, T.; Muck-Lichtenfeld, C. *Org. Biomol. Chem.* **2007**, *5*, 741−758.
(31) Van Lenthe, E.; Baerends, E. J. *J. Comput. Chem.* **2003**, *24*, 1142−1156.
(32) Downs, R. T.; Hall-Wallace, M. *Am. Mineral.* **2003**, *88*, 247−250.
(33) Wolinski, K.; Hinton, J. F.; Pulay, P. *J. Am. Chem. Soc.* **1990**, *112*, 8251−8260.
(34) Schreckenbach, G.; Ziegler, T. *J. Phys. Chem.* **1995**, *99*, 606−611.
(35) Schreckenbach, G.; Ziegler, T. *Int. J. Quantum Chem.* **1997**, *61*, 899−918.
(36) Wolff, S. K.; Ziegler, T. *J. Chem. Phys.* **1998**, *109*, 895−905.
(37) Wolff, S. K.; Ziegler, T.; van Lenthe, E.; Baerends, E. J. *J. Chem. Phys.* **1999**, *110*, 7689−7698.
(38) Luca, V.; Thomson, S.; Howe, R. F. *J. Chem. Soc., Faraday Trans.* **1997**, *93*, 2195−2202.
(39) Das, N.; Eckert, H.; Hu, H.; Wachs, I. E.; Walzer, J. F.; Feher, F. J. *J. Phys. Chem.* **1993**, *97*, 8240−8243.
(40) Kalinkin, P.; Kovalenko, O.; Lapina, O.; Khabibulin, D.; Kundo, N. *J. Mol. Catal. A: Chem.* **2002**, *178*, 173−180.
(41) Wachs, I. E. *Dalton Trans.* **2013**, *42*, 11762−11769.

DOI: 10.1021/acscatal.5b00286
ACS Catal. 2015, 5, 3945−3952